ACS SyntheticBiology

Letter

pubs.acs.org/synthbio

Refactored M13 Bacteriophage as a Platform for Tumor Cell Imaging and Drug Delivery

Debadyuti Ghosh,[‡,§,∥,#] Aditya G. Kohli,[†,‡,∥,¶,#] Felix Moser,[†] Drew Endy,[⊥] and Angela M. Belcher*[,†,‡,§,∥]

[†]Department of Biological Engineering, [‡]The David H. Koch Institute for Integrative Cancer Research, and [§]Department of Materials Science and Engineering, Massachusetts Institute of Technology, Cambridge, Massachusetts, United States

[∥]MIT-Harvard Center of Cancer Nanotechnology Excellence, Cambridge, Massachusetts, United States

[⊥]Department of Bioengineering, Stanford University, Stanford, California, United States

Supporting Information

ABSTRACT: M13 bacteriophage is a well-characterized platform for peptide display. The utility of the M13 display platform is derived from the ability to encode phage protein fusions with display peptides at the genomic level. However, the genome of the phage is complicated by overlaps of key genetic elements. These overlaps directly couple the coding sequence of one gene to the coding or regulatory sequence of another, making it difficult to alter one gene without disrupting the other. Specifically, overlap of the end of gene VII and the beginning of gene IX has prevented the functional genomic modification of the N-terminus of p9. By redesigning the M13 genome to physically separate these overlapping genetic elements, a process known as "refactoring," we enabled independent manipulation of gene VII and gene IX and the construction of the first N-terminal genomic modification of p9 for peptide display. We demonstrate the utility of this refactored genome by developing an M13 bacteriophage-based platform for targeted imaging of and drug delivery to prostate cancer cells *in vitro*. This successful use of refactoring principles to re-engineer a natural biological system strengthens the suggestion that natural genomes can be rationally designed for a number of applications.

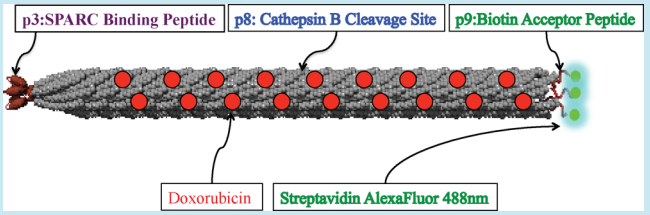

KEYWORDS: *genome refactoring, drug delivery, M13 bacteriophage, synthetic biology*

Recent advances in synthetic biology have led to the development of a number of rationally designed therapeutic platforms, including cancer-targeting bacteria and an adenovirus-based detection of aberrant p53 signaling.[1,2] M13 bacteriophage is another attractive therapeutic platform because of its ability to display peptides and the strong fundamental understanding of its biology.[3,4] Its strength as a phage display platform is derived from its straightforward propagation in bacteria and facile isolation of single-stranded viral DNA for sequencing or mutagenesis. Peptide display is based on the ability to genetically engineer short (6−15 amino acids) peptides to the terminal ends of phage coat proteins, which are then presented on the surface of the phage. Phage displaying peptides with strong affinities to target materials or biomolecules can then be selectively enriched and propagated from a randomized display library. This high-throughput platform has facilitated the discovery of peptide motifs with strong affinities to epitopes,[3,5] antibodies,[6] and mammalian cells.[7−9] Our laboratory has also displayed multiple peptides on M13 to grow and nucleate various inorganic materials.[10−17]

In practice, the utility of M13 for peptide display is partly determined by the ability to manipulate the phage genome without excessively disrupting phage function, as display peptides are genetically fused directly to phage coat proteins. However, the manipulation of the phage genome is greatly limited by the presence of overlapping gene regions. These overlapping regions limit the creation of peptide fusions with phage coat proteins, since insertion of such a peptide sequence at one end of a protein sequence will disrupt the coding and regulatory region of the adjacent gene. For example, the gene VII stop codon overlaps with the start codon of gene IX. Also, the ribosome-binding site (RBS) that regulates gene IX is embedded in the coding region of gene VII. This sharing of critical sequence elements makes it impossible to manipulate one gene without disrupting the other. Indeed, the overlap of coding sequences and regulatory elements at the DNA level often confound attempts to rationally engineer gene expression in higher organisms (C. Voigt, personal correspondence).

One approach to remedy this problem was developed by Endy and co-workers, who set out to "refactor" the T7 bacteriophage genome by physically separating genetic elements and bracketing them with endonuclease sites to enable further modification.[18] In this work, the viable refactoring of the T7 phage genome enabled easier study and manipulation of the phage and provided a proof-of-concept that genomes can be rationally and systematically redesigned. Nonetheless, the benefits of refactoring have remained unclear

Received: June 4, 2012
Published: August 17, 2012

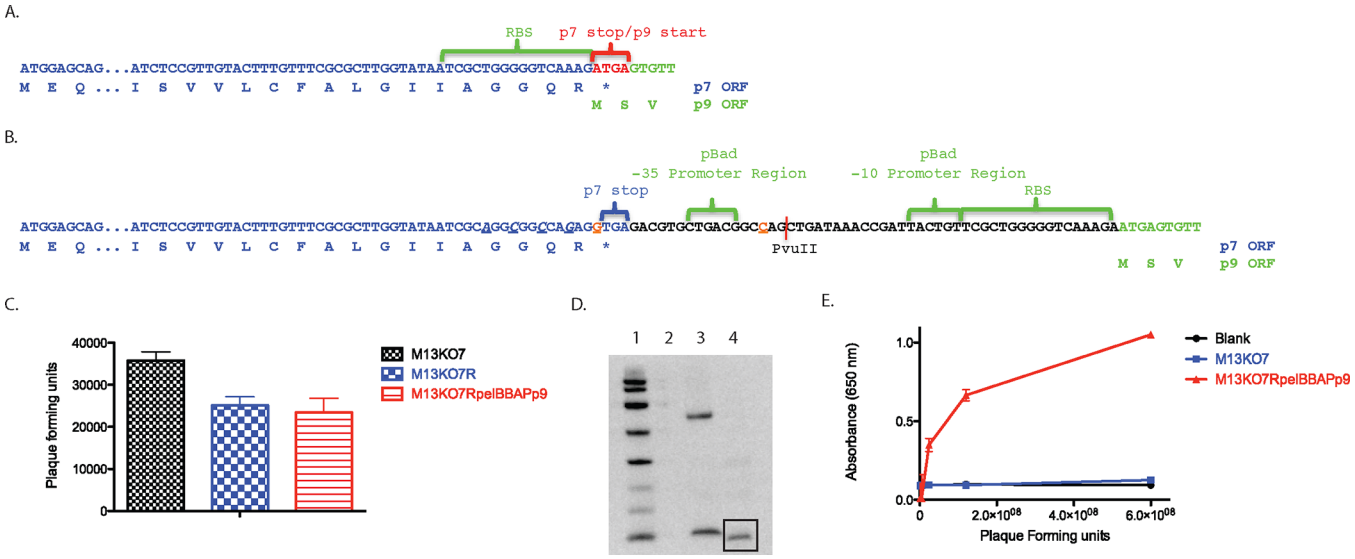

Figure 1. M13KO7 refactoring and phage characterization. DNA and protein sequences for gene VII−gene IX junction are shown before and after redesign. (A) M13K07 "wild-type" gene VII/gene IX overlap. (B) The refactored M13KO7R gene VII/gene IX overlap is shown. In the wild-type sequence (A), the gene IX RBS are present at the C-terminus of gene VII and the stop codon for p7 overlaps with the start codon for p9. In the refactored sequence (B), the gene IX RBS was duplicated and shifted upstream of the gene IX start codon. A pBAD promoter was introduced upstream of the gene IX start codon. The native gene IX RBS (denoted) and start codon (underlined, orange) were silenced and a PvuII endonuclease site (underlined, orange) was introduced. (C) Phage infectivity assay. Equivalent, serial 10-fold dilutions of native M13KO7, M13KO7R, and M13KO7RpelBBAPp9 phage were incubated with ER2738 and plated with agar overlay. Samples were run in triplicate and error bars represent standard deviations. (D) Western blot of biotinylated p9. To confirm p9 expression, biotin acceptor peptide (BAP) was fused to the p9 N-terminus of M13 phage (previously denoted as M13KO7pelBBAPp9) and was enzymatically biotinylated. M13KO7pelBBAPp9 virions (lane 4) were run on gel electrophoresis against negative control M13KO7R phage without BAP (lane 2), a positive control (lane 3), and sizes were compared to a biotinylated ladder (lane 1). Samples were blotted, probed with a streptavidin conjugate and visualized. A small band is observed in the M13KO7pelBBAPp9 sample around 6.15 kD, which is the expected molecular weight of the fusion p9 protein. (E) ELISA of biotinylated, redesigned p9 phage. To confirm functionality of re-engineered p9, biotinylated M13KO7pelBBAPp9 phage were tested for binding to streptavidin compared to that of negative control M13 and blank samples. Samples were probed with a phage-specific antibody and incubated with chromogenic substrate. Absorbances were measured at 650 nm. All samples were run in triplicate and error bars represent standard deviations.

due to the difficulty of the process and the lack of examples of refactoring enabling novel functionality or utility.

Here, we demonstrate that refactoring can increase the utility of M13 bacteriophage for phage display. We redesigned the M13 bacteriophage genome by physically decoupling the genetic elements at the gene VII/gene IX overlap. This decoupling allowed for N-terminal genomic modification of protein p9 that was not previously possible without the use of a phagemid system. We demonstrate that the refactored phage remained viable and that the displayed peptides are functional. Finally, we show the utility of the refactored genome by recasting the phage as a vector for cancer drug delivery and imaging. To our knowledge, this is the first example of display using the genomic copy of protein p9 and the first demonstrated application of genome refactoring.

Refactoring the Gene VII/Gene IX Overlap. The goal of refactoring is to improve the internal structure of a system such that it is easier to engineer.[18] In this study, we sought to enhance the utility of M13 bacteriophage as a platform for multiple peptide display by partially refactoring its genome at the gene VII/gene IX overlap. Genes VII and IX both produce critical structural proteins that are necessary for viable phage assembly. Genomic modifications of genes VII and IX in this region have been prohibited by the overlap of the start codon of gene IX with the stop codon of gene VII (Figure 1A). Additionally, the presence of the gene IX ribosome binding site (RBS) in the gene VII coding region makes gene IX expression dependent on gene VII coding. Thus, any peptide sequences fused to the beginning of gene IX or end of gene VII will disrupt functional expression of the other gene and prevent proper phage assembly. This overlap has limited display of peptides on p9 and highlights the need for refactoring of this region. To decouple gene IX from gene VII, we first introduced a silent mutation (A1206G) in order to knock out the native start codon for p9 (Figure 1B). Next, we inserted a leaky pBAD promoter immediately between the gene VII stop codon and a new gene IX start codon, as no native p9 promoter is known. The gene IX RBS was incorporated upstream of the new gene IX start codon, and the native RBS was disrupted by silent codon shuffling in order to prevent direct repeats that would be vulnerable for deletion by the phage. In addition to decoupling the two genes, a number of restriction sites were engineered as silent mutations into the platform to allow for further manipulation of the genome (see Methods). All of the above modifications combined to form the refactored M13K07R plasmid. We tested the viability and infectivity of the engineered virions as compared to the wild-type phage (M13KO7). M13KO7R phage formed viable phage with titers similar to that of M13KO7 phage (Figure 1C); there is an approximate 1.4-fold decrease in phage titer output with M13KO7R compared to M13KO7. Previous work confirmed that gene overlaps in viruses increase the stability of viruses by reducing the incidence of mutation and sequence redundancy.[19] However, our initial findings suggest that while genome overlaps may be evolutionarily favorable, they are not necessary for phage viability.

Refactored M13 Is Capable of p9Modification and Peptide Display. As described above, peptide fusions to the

dx.doi.org/10.1021/sb300052u | ACS Synth. Biol. 2012, 1, 576−582

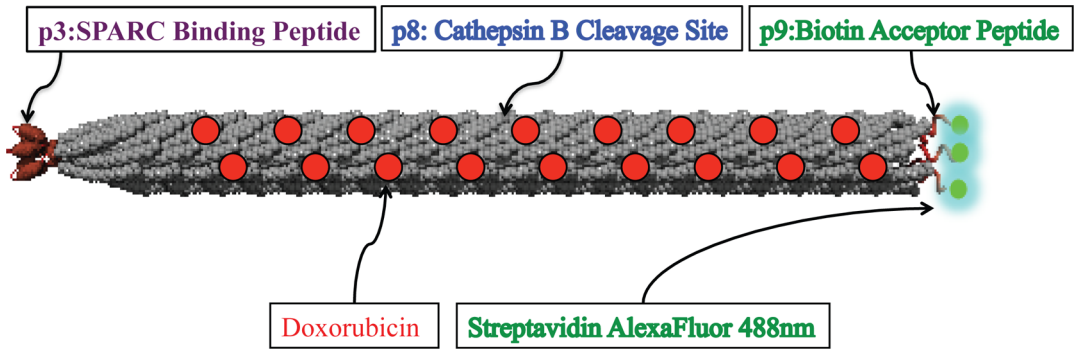

Figure 2. Schematic of M13-983 Phage. (A) The red dots along the phage coat represent DOX attached to p8. p3 displays a peptide with affinity for SPARC, and p9 can be enzymatically biotinylated and loaded with streptavidin-functionalized fluorophores.

N-terminus of the p9 protein on wild-type M13 are difficult to make because of the overlap between genes VII and IX. As such, the only viable gene IX modifications have relied on a phagemid system,[20] which uses a second copy of gene IX on a plasmid to produce a modified version of p9 that gets incorporated into the M13 capsid. However, a phagemid system prohibits the production of a homogeneous population of phage (Supplementary Figure 1), since both the wild-type and modified version of the protein are incorporated in the phage coat. Also, previous work with fusion display on major coat p8 has shown the length and sequence of the fusion peptide or protein can affect the efficiency of display on phage capsid proteins.[21] As such, the wild-type phage protein is often more readily incorporated into the phage coat, and only a small proportion of the phage population contains the modified version. Therefore, modifying coat proteins at the genomic level guarantees a homogeneous population of phage that incorporates only the modified version of the protein.

To demonstrate the ability of the refactored M13 genome to produce homogeneous populations of tagged p9 phage, we sought to create the first genomic modification of the N-terminus of p9 and use the resulting phage for tumor targeting and imaging. Refactored p9 was modified for N-terminal display of a biotin acceptor peptide (BAP) (Figure 2A). BAP is a 15-amino-acid peptide substrate (GLNDIFEAQKIEWHE) that can be enzymatically biotinylated at its lysine residue by birA biotin protein ligase.[22] The biotinylated peptide acts as a handle to which a myriad of streptavidin-functionalized moieties can be conjugated site-specifically to the phage, taking advantage of the strong noncovalent biotin−avidin interaction. Upstream of the BAP sequence, a pelB leader signal sequence was inserted to ensure proper incorporation of BAP-p9 into the phage coat during replication and assembly.[23] Genome engineering of gene IX allows for display of fusion p9 without the need for a phagemid system.

The production and infectivity of the resulting M13K07RpelBBAPp9 phage were assessed by spectrophotometry and titering. The number of phage particles can be quantified by UV−vis spectrophotometry.[24] After amplification, M13KO7RpelBBAPp9, M13KO7, and M13KO7R showed similar phage yields (Supplementary Figure 2), demonstrating that phage amplification in bacteria was unaffected by genome modification. Phage infectivity was quantified by a plaque formation assay. Unmodified M13KO7 had a titer approximately 1.4-fold higher than that of refactored M13KO7R and M13KO7RpelBBAP, while M13KO7R and M13KO7RpelBBAPp9 had comparable titers (Figure 1C). This result confirms the viability of the modified M13KO7 clones. There is little difference in phage infectivity or production between the M13KO7 and refactored clones. This finding suggests that insertion of the pelB leader and BAP sequences does not significantly affect phage production and is in line with known phage biology. p9 is believed to play a role in the initiation of phage assembly and is not involved in bacterial infection.[25] Further, p9 is believed to be present in stoichiometric excess during assembly.[25] As such, moderate variations in p9 levels should not impact infectivity or phage production. This result demonstrates that refactored p9 is modular and can tolerate insertion of heterologous peptides.[23,26] To assess the functionality of BAP-p9 fusion, BAP-p9 expression and subsequent biotinylation was confirmed by enzymatically biotinylating M13K07RpelBBAPp9 and then running the phage on an SDS gel. The blot was probed for biotinylated proteins using a streptavidin conjugate. The presence of a band at 6.15 kD, which is the expected molecular weight of the fusion BAP-p9, suggests proper expression and biotinylation of fusion BAP-p9 (Figure 1D, lane 4). In order to test functionality of p9, biotinylated phage was assayed for streptavidin binding by ELISA. M13K07pelBBAPp9 binding to streptavidin increased with increased titers, as measured by absorbance ($OD_{650\ nm}$), whereas wild-type M13 showed no correlation, suggesting that biotinylated phage is both viable and capable of binding streptavidin (Figure 1E). This M13K07RpelBBAPp9 construct represents the first viable genomic fusion of the p9 coat protein.

Refactored M13 Enables Cancer Cell Targeting, Imaging, and Drug Delivery. We sought to take advantage of the refactored phage's ability to display multiple peptides at once to engineer the phage for tumor targeting, imaging, and drug delivery. Targeted drug delivery vehicles offer improved safety and efficacy profiles over traditional chemotherapeutics by concentrating drug at the tumor site and limiting off-target toxicities. A number of nanoparticle drug carriers are used in the clinic and are in development;[27] however, few allow for simultaneous drug delivery and tumor imaging.

To further engineer M13 for tumor cell targeting and drug delivery, the M13SK vector[10] was engineered to display peptides on p3 and p8. To facilitate tumor targeting, the p3 phage coat protein was fused to the SPARC (Secreted Protein, Acidic and Rich in Cysteine) Binding Peptide (SBP) sequence SPPTGIN.[28] SPARC, an anti-adhesive and promigratory matricellular glycoprotein, is overexpressed in aggressive melanoma, breast, brain, prostate, colon, and lung cancers.[29] For proof of concept of refactored M13 as a drug delivery vehicle, we loaded the phage with doxorubicin (DOX), a potent

dx.doi.org/10.1021/sb300052u | ACS Synth. Biol. 2012, 1, 576−582

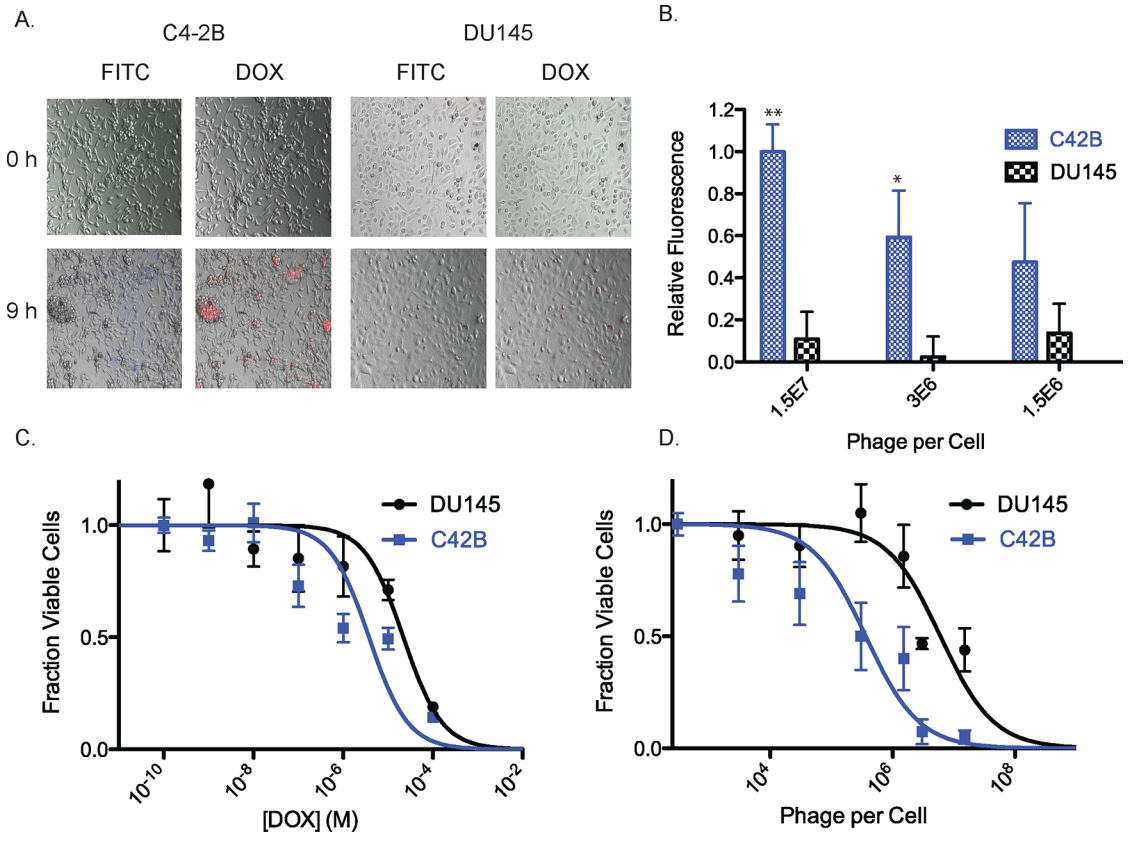

E.

	C42B IC_{50}	DU145 IC_{50}
Free DOX (μM DOX)	3.7 (.72 to 19.5)	22.0 (7.2 to 66.8)
M13-983-Alexa-DOX (Phage per cell)	3.6E5 (1.8E5 to 7.0E5)	6.1E6 (3.7E6 to 9.9E6)
M13-983-Alexa-DOX (μM DOX Equivalents)*	.05 (.02 to .1)	.86 (.52 to 1.4)

Figure 3. Simultaneous imaging and therapy of SPARC positive tumor cells. (A) Overlay of brightfield and fluorescent images of SPARC positive C42B cells (first and second column) and less expressing SPARC DU145 cells (third and fourth column) incubated with M13-983-Alexa-DOX at 0 h (top row) and 9 h post-treatment (bottom row). FITC channel represents fluorescence from Alexa Fluor 488, and DOX is designated by red fluorescence from DOX uptake. C42B samples showed increased fluorescence of phage uptake, indicated by green fluorescence (bottom row, first column) and DOX uptake (bottom row, second column) as compared to DU145 cells after 9 h. (B) Targeted uptake measured by quantifying fluorescence intensity (**$P < 0.001$; *$P < 0.01$). C42B consistently shows higher fluorescence intensity than DU145, confirming the observations in panel A. Higher phage concentrations report larger differences between C42B and DU145 fluorescence. (C) Cell viability of C42B and DU145 as a function of free DOX. (D) Cell viability of C42B and DU145 cell lines as a function of increasing M13-983-Alexa-DOX. All samples were run in triplicate and error bars represent standard deviations. (E) IC_{50} values for C42B and DU145 are given with the 95% confidence interval given in parenthesis. *Based on 257 DOX particles per phage.

chemotherapeutic used extensively in the clinic. To facilitate DOX release, the p8 phage coat protein was fused to the peptide motif DFK. This peptide sequence is recognized by cathepsin B, a lysosomal cysteine protease. This modification should allow for intracellular drug release, as cathepsin-B is overexpressed in prostate cancer.[30] DOX was conjugated to the aspartic acid residue of p8 by EDC coupling, and DOX loading was quantified by reading the absorbance of the phage−drug conjugate at 490 nm. Each phage carried an average of 257 DOX molecules, which suggests that less than 10% of the 2700 copies of the p8 coat protein are functionalized with DOX. The SBP and DFK modified M13 was further modified by introduction of a NheI restriction endonuclease site downstream of gene IX to facilitate transfer of the refactored pelB-BAP-p9 sequence into the SBP and DFK modified M13. The resulting phage, named M13-983, displays BAP at p9, DFK at p8, and SBP at p3 (Figure 2). To functionalize M13-983 for imaging, the phage was enzymatically biotinylated on p9-BAP and incubated with streptavidin-coated AlexaFluor 488 nm dye to form M13-983-Alexa-DOX phage (Figure 2).

To assess cell targeting, M13-983-Alexa-DOX phage was added to human prostate cancer cell lines expressing either SPARC (C42B) or low levels of SPARC (DU145). At 9 h post-treatment, C42B cells demonstrated Alexa Fluor 488 (green) and intrinsic DOX (red) fluorescence (Figure 3A, second row, first and second column), while DU145 cells exhibited minimal fluorescence from phage-DOX uptake (Figure 3A, second row, third and fourth column). At 9 h, DOX uptake was observed in

dx.doi.org/10.1021/sb300052u | ACS Synth. Biol. 2012, 1, 576−582

rounded C42B cells, as indicated by the overlaid red fluorescence (Figure 3A, second row, second column). While the DU145 cells looked healthy from 0 to 9 h post-treatment, the C42B cells were more rounded and surrounded by cellular debris (Figure 3A, second row, first and second columns), possibly indicating that they were undergoing DOX-mediated cell death. At several different concentrations of M13-983-Alexa-DOX, the normalized fluorescence intensity is about 10 times greater on SPARC positive C42B cells than DU145 cells (Figure 3B). This result demonstrates effective targeting of the phage to SPARC as well as the imaging capabilities of the M13 platform. Both DU145 and C42B cells incubated with phage not functionalized with DOX showed no noticeable toxicity (Supplementary Figure 3).

After confirming targeting, we assessed the cytotoxic potential of M13-983-Alexa-DOX. Immediately after imaging, cells were allowed to recover in media for 14 h at 37 °C. The cytotoxicity of the M13-983-Alexa-DOX platform was then evaluated using an MTT assay. Cell viability decreased with increasing concentrations of M13-983-Alexa-DOX (Figure 3D,E). In addition, this complex killed SPARC positive C42B cells ~20 times more efficiently than control DU145, demonstrating targeted drug delivery. From the IC_{50}, this complex was ~100 times more cytotoxic than free doxorubicin (Figure 3C,E) and thus serves to reduce the effective DOX dose (Figure 3E).

Here we outline how refactoring of the M13 phage genome has enabled simultaneous prostate cancer cell imaging and targeted drug delivery. By decoupling gene VII and gene IX on the M13 genome, the p9 protein can be modified at its N-terminus without disrupting the p7 coding region. This system obviates the need for a phagemid and enables the production of a viable and homogeneous phage population. By using the refactored phage to display peptides at p9, p8, and p3 simultaneously and by attaching imaging and drug moieties to p9 and p8, we demonstrate specific imaging and therapy of tumor cells *in vitro*. This is the first example of N-terminal genomic modification of p9 and subsequent application of genome refactoring.

Refactoring of the geneVII/geneIX region and subsequent fusion of BAP to p9 had minimal effect on phage viability. Interestingly, refactoring does not dramatically decrease the viability of the phage. Recent work investigating various subtypes of DNA and RNA viruses suggests that physical constraint of the protein coat and its organization may be responsible for genome compression and subsequent gene overlaps.[31] However, it is known that the size of the phage coat is plastic. Shrinking the genome of wild-type phage from 6.4 kb to 221 bp changed the phage coat composition from 2700 to 95 copies of p8.[32] Further, expansion of the genome can result in phage particles with larger p8 coats.[33] As such, the plasticity in the phage coat may compensate for the expanded phage genome with no consequences in phage assembly, and re-engineering the genome may not be as deleterious as previously considered. However, future work is needed to characterize and fully elucidate the exact role of gene overlaps in filamentous phage.

This phage platform is modular and easily modifiable for a number of applications. In these proof-of-concept studies, we used Alexa Fluor 488 as an imaging agent; however, any streptavidin-functionalized moiety can be attached to p9. Recent work in the laboratory has incorporated various epitope tags including against hemagglutinin into refactored p9 for applications including purification and site-specific labeling (data unpublished). DOX can be replaced with other small molecule drugs with a free amine group. Further, the tropism of the phage can be directed to different tumor types and tumor markers by switching the targeting peptide encoded in gene III.

There is much to be gained by further optimizing the refactored platform and understanding the behavior of the re-engineered phage. Successfully decoupling gene VII and gene IX has allowed for facile N-terminal peptide display on p9; however, other genes overlap in the M13K07 plasmid, most notably, gene IX and gene VIII. Further refactoring of these genes and introduction of flanking restriction sites will allow for more complete modification of the M13K07 platform. This work suggests the potential of redesigning evolved biological systems to confer new, additional, and enhanced functionalities for possible therapy and imaging.

METHODS

Refactoring p9 and p7 of M13. M13KO7 (New England Biolabs, Beverly, MA) was used as the template to refactor overlapping p9 and p7 DNA sequences. The following eight unique restriction sites were introduced into M13KO7 using multi site-directed mutagenesis (Agilent Technologies) for easier re-engineering of the phage: XbaI (C165T), MluI (A351T), Bsu36I (T564A), MfeI (C718T), NheI (CTCT to TAGC starting at 1232), BglI (A1333G), BlpI (T1653C), *Eco*RI (T2598G). These restriction sites resulted in silent mutations for encoded proteins and did not alter any known promoters or ribosome binding sites. A 272 bp synthetic DNA sequence encoding the refactored region described in the text was then generated by DNA2.0 and inserted between sites BsrGI and NheI by standard endonuclease cloning (Supplementary Figure 4, Genbank accession JN712255). Plasmid maps were prepared using Geneious v4.8.

Engineering p9 for N-Terminal Display. Using elements of refactored p9, a gene part was constructed using *de novo* DNA synthesis (DNA2.0, CA) with a pelB leader sequence directly upstream of DNA of p9 fused to a gold binding peptide (GBP)[34] flanked by BsrGI and NheI restriction sites. The resulting pelB signal peptide will direct the fusion p9 into the *E. coli* periplasm for recombinant phage assembly. The pelB-GBP-p9 sequence was cut with BsrGI/NheI and engineered into the corresponding sites in refactored M13KO7R to form M13KO7RpelBGBPp9. For further studies, the sequence for the gold binding peptide was excised with SfiI and the DNA sequence for biotin acceptor peptide (BAP) was genetically engineered, resulting in M13KO7RpelBBAPp9. BAP is a 15-amino-acid peptide (GLNDIFEAQKIEWHE) that is site-specifically biotinylated at its lysine residue.[22]

Construction of M13 Vector for p3/p8 Display. M13SK was used for dual display of peptides on p3 and p8, as described previously.[10] *Pst*I and *Bam*HI sites were engineered into M13KE (purchased from NEB) by site-directed mutagenesis (T1372A and C1381G, respectively) enabling genetic manipulation of p8 for N-terminal peptide display, and the *Pst*I site at 6250 was knocked out by mutation (A6250T). The resulting vector, M13SK, was amenable for p3 and p8 display by direct cloning into the phage genome. SPARC binding peptide (SPPTGIN) was engineered into the N-terminus of p3 for display. Briefly, oligonucleotides encoding for SBP, 5′ GTA CCT TTC TAT TCT CAC TCT TCA CCA CCG ACT GGA ATT AAC GGA GGC GGG TC 3′ and 5′ GGC CGA CCC GCC TCC GTT AAT TCC AGT CGG TGG TGA AGA

GTG AGA ATA GAA AG-3′ (Operon, AL), were annealed, phosphorylated, and cloned into the Acc65I and EagI sites of M13SK. To display the cathepsin protease cleavage motif DFK,[35] 5′ GAT TTC AAG 3′ and 5′ GAT CCT TGA AAT CTG CA-3′ were annealed, phosphorylated, and engineered into the *Pst*I and *Bam*HI sites. All sequences were confirmed by DNA sequencing by Koch Institute Swanson Biotechnology Center. The pelB-BAP-p9 sequence was excised from the M13K07R scaffold using BsrGI/NheI endonucleases and incorporated into the M13SK-SBP-DFK construct, resulting in the final vector M13-983 (Supplementary Figure 5, Genbank accession JN790190). M13-983 was transformed into XL-1 Blue chemical competent cells (Agilent Technologies), mixed with agarose top, and plated on LB-agar plates with 20 μg/mL tetracycline, isopropyl β-D-1-thiogalactopyranoside (IPTG), and X-gal. Blue plaques were picked, and DNA was isolated and sequenced to confirm final construct.

Phage Amplification and Purification. To amplify M13-983 phage for phage-based experiments, a culture of ER2738 (NEB), a F-pilus positive *E. coli* strain, was grown overnight in tetracycline antibiotic. The following day, a freshly picked plaque of M13-983 was grown in a 1:100 dilution of ER2738 in selective media to midlog phase (~4.5−5 h). Cultures were centrifuged at 10,000 rpm for 15 min. Supernatants were collected, and phage were precipitated overnight at 4 °C with PEG 8000/2.5 M NaCl. After centrifugation, phage was resuspended in 1 mL of PBS and titered by UV−vis spectrometry or plaque forming assay.

Biotinylation of M13-983. M13-983 phage was enzymatically biotinylated using an *in vitro* biotinylation kit from Avidity and adapting from manufacturer's recommendations. Briefly, 1 × 10^{14} pfu phage were resuspended in 620 μL of PBS and mixed with 80 μL of Biomix-A, 80 μL of Biomix-B, and 20 μL of birA biotin protein ligase for site-specific biotinylation on the lysine residue of the BAP sequence. Reactions were incubated for 12 h at 30 °C. After, phage were PEG-precipitated twice and resuspended in 1 mL of PBS.

Western Blotting and ELISA for BAP Functionality on Re-engineered p9. p9 expression and functionality were confirmed by Western blotting and ELISA. For Western blotting, 1 × 10^{12} pfu control and biotinylated phage, along with a biotinylated ladder (BioRad, CA), were run on a 4−12% NuPage Bis-Tris Acetate Mini Gel (Invitrogen, CA) under denaturing conditions. Samples were transferred onto a PVDF membrane (Invitrogen), blocked with 5% BSA-PBS, washed, and probed with 1:50000 dilution of anti-M13 horseradish peroxidase conjugate (GE Life Sciences, CA) for detection. To confirm p9 functionality, biotinylated p9 was tested for binding to streptavidin. Serial 5-fold dilutions of biotinylated p9 phage and negative control M13 were bound to microtiter plates coated with 1 mg/mL NeutrAvidin (Pierce, CA). After 1 h of incubation, wells were washed, blocked, and probed with anti-M13-HRP to probe for phage binding. TMB (3,3′,5,5′-tetramethylbenzidine) was added to wells, and absorbance was measured at 652 nm using a SpectraMax M2e plate reader (Molecular Devices, CA). All samples were run in triplicate.

Conjugation for Imaging and Therapy *in Vitro*. A total of 1 × 10^{14} phage were enzymatically biotinylated and incubated with 100 μL of 1 mg/mL Streptavidin-Alexa Fluor 488 for 1 h at room temperature under gentle mixing. Phage were PEG-precipitated twice and resuspended in 500 μL of PBS for further drug conjugation. Doxorubicin (DOX) hydrochloride was purchased from Sigma-Aldrich, and EDC and Sulfo-NHS were purchased from Thermo Scientific. A 0.4 mg portion of EDC and 1.1 mg of sulfo-NHS were incubated with 10^{13}/mL M13-983-Alexa for 15 min in 3x EDC activation buffer (0.3 M MES, 1.5 M NaCl, pH 6.0). The EDC reaction was quenched with 20 mM 2-mercaptoethanol (Thermo Scientific). DOX was added at 50−100 μg/mL for the conjugation reaction, and the reaction was allowed to proceed for 2 h at room temperature in a fume hood. The conjugation was quenched with 10 mM hydroxylamine to hydrolyze unreacted NHS and regenerate original carboxyl groups. After conjugation, the reactions were dialyzed against PBS for 2 days using dialysis membrane, MWCO of 12,000−14,000, (SpectraLabs) with frequent buffer exchange. The amount of DOX per phage was measured by UV−vis at 490 nm.

Imaging and Cytotoxicity Assay. To evaluate cytotoxicity, M13-983-Alexa-DOX was incubated with C4-2B and DU145 cells for 9 h at 37 °C in 50% DPBS, 50% PBS. Cells were seeded at 33,000 cells/well in a 96-well tissue culture microtiter plate. Complexes were removed, and cells were washed with PBS. Cells were imaged using an Olympus IX51 inverted microscope (Olympus, WA) under the 485/538 excitation/emission filter. Quantitative fluorescent measurements were obtained using a plate reader (excitation 485 nm, emission 538 nm). Images were captured using camera software and overlaid and processed using NIH ImageJ software. After imaging cells were grown for 14 h in complete DMEM or TMEM. An MTT assay was used to measure cell viability. Samples were measured in triplicate.

Cell Lines and Culture. DU145 and C4-2B human prostate cancer cell lines were provided courtesy of Dr. Kimberly Kelly (University of Virginia). DU145 was grown in Dulbecco's Minimum Essential Medium (DMEM) supplemented with 10% fetal bovine serum (FBS) (Hyclone, Logan, UT) and 1% penicillin/streptomycin (Invitrogen, CA) at 37 °C in 5% CO_2. C4-2B were grown in T-medium (Invitrogen) with 10% FBS and penicillin/streptomycin. LNCaP were grown in RPMI medium (without phenol red), supplemented with 10% FBS, 1% penicillin/streptomycin, 1% sodium pyruvate, and 1% HEPES buffer.

■ ASSOCIATED CONTENT

Supporting Information

Supplementary data, figures, and plasmid maps. This material is available free of charge via the Internet at http://pubs.acs.org.

■ AUTHOR INFORMATION

Corresponding Author

*Ph: (617) 252 1163. E-mail: belcher@mit.edu.

Present Address

[¶]UC Berkeley and UCSF Graduate Program in Bioengineering, California.

Author Contributions

[#]These authors contributed equally to this work.

Author Contributions

D.G., A.G.K., D.E., and A.M.B. conceived the idea. D.G., A.G.K., F.M., and D.E. designed the refactored M13 genome and re-engineered p9. D.G. and A.G.K. made the subsequent engineered p9 constructs. F.M. made the M13KO7R construct. D.G. and A.G.K. performed all of the experiments shown in the results. D.G., A.G.K., F.M., D.E., and A.M.B. wrote the paper.

Notes

The authors declare no competing financial interest.

■ ACKNOWLEDGMENTS

This work was funded by the National Cancer Institute Center for Cancer Nanotechnology Excellence (U54-CA119349-04) and the National Science Foundation Synthetic Biology Engineering Research Center (SynBERC). We would like to thank Koch Institute Swanson Biotechnology Center for help with sequencing.

■ REFERENCES

(1) Anderson, J., Clarke, E., Arkin, A., and Voigt, C. (2006) Environmentally controlled invasion of cancer cells by engineered bacteria. *J. Mol. Biol. 355*, 619−627.

(2) Ramachandra, M., Rahman, A., Zou, A., Vaillancourt, M., Howe, J. A., Antelman, D., Sugarman, B., Demers, G. W., Engler, H., Johnson, D., and Shabram, P. (2001) Re-engineering adenovirus regulatory pathways to enhance oncolytic specificity and efficacy. *Nat. Biotechnol. 19*, 1035−1041.

(3) Scott, J. K., and Smith, G. P. (1990) Searching for peptide ligands with an epitope library. *Science 249*, 386−390.

(4) Rosenberg, A., Griffin, K., and Studier, F. (1996) T7Select Phage Display System: A powerful new protein display system based on bacteriophage T7. *Innovations*, 1−6.

(5) Smith, G. P. (1985) Filamentous fusion phage: novel expression vectors that display cloned antigens on the virion surface. *Science 228*, 1315−1317.

(6) Parmley, S. F., and Smith, G. P. (1988) Antibody-selectable filamentous fd phage vectors: affinity purification of target genes. *Gene 73*, 305−318.

(7) Barry, M. A., Dower, W. J., and Johnston, S. A. (1996) Toward cell-targeting gene therapy vectors: selection of cell-binding peptides from random peptide-presenting phage libraries. *Nat. Med. 2*, 299−305.

(8) Pasqualini, R., and Ruoslahti, E. (1996) Organ targeting in vivo using phage display peptide libraries. *Nature 380*, 364−366.

(9) Ghosh, D., and Barry, M. A. (2005) Selection of muscle-binding peptides from context-specific peptide-presenting phage libraries for adenoviral vector targeting. *J. Virol. 79*, 13667−13672.

(10) Dang, X., Yi, H., Ham, M. H., Qi, J., Yun, D. S., Ladewski, R., Strano, M. S., Hammond, P. T., and Belcher, A. M. (2011) Virus-templated self-assembled single-walled carbon nanotubes for highly efficient electron collection in photovoltaic devices. *Nat. Nanotechnol. 6*, 377−84.

(11) Lee, S.-W., Mao, C., Flynn, C. E., and Belcher, A. M. (2002) Ordering of quantum dots using genetically engineered viruses. *Science 296*, 892−895.

(12) Lee, Y. J., Yi, H., Kim, W.-J., Kang, K., Yun, D. S., Strano, M. S., Ceder, G., and Belcher, A. M. (2009) Fabricating genetically engineered high-power lithium-ion batteries using multiple virus genes. *Science 324*, 1051−1055.

(13) Mao, C., Qi, J., and Belcher, A. M. (2003) Building quantum dots into solids with well-defined shapes. *Adv. Funct. Mater. 13*, 648−656.

(14) Mao, C., Flynn, C. E., Hayhurst, A., Sweeney, R., Qi, J., Georgiou, G., Iverson, B., and Belcher, A. M. (2003) Viral assembly of oriented quantum dot nanowires. *Proc .Natl. Acad. Sci. U.S.A. 100*, 6946−6951.

(15) Mao, C., Solis, D. J., Reiss, B. D., Kottmann, S. T., Sweeney, R. Y., Hayhurst, A., Georgiou, G., Iverson, B., and Belcher, A. M. (2004) Virus-based toolkit for the directed synthesis of magnetic and semiconducting nanowires. *Science 303*, 213−217.

(16) Nam, K. T., Kim, D.-W., Yoo, P. J., Chiang, C.-Y., Meethong, N., Hammond, P. T., Chiang, Y.-M., and Belcher, A. M. (2006) Virus-enabled synthesis and assembly of nanowires for lithium ion battery electrodes. *Science 312*, 885−888.

(17) Yi, H., Ghosh, D., Ham, M. H., Qi, J., Barone, P. W., Strano, M.-S., and Belcher, A. M. (2012) M13 phage-functionalized single-walled carbon nanotubes as nanoprobes for second near-infrared window fluorescence imaging of targeted tumors. *Nano Lett. 12*, 1176−1183.

(18) Chan, L. Y., Kosuri, S., and Endy, D. (2005) Refactoring bacteriophage T7. *Mol. Syst. Biol. 1*, 1−10.

(19) Krakauer, D. (2002) Evolutionary principles of genomic compression. *Comments Theor. Biol. 7*, 215−236.

(20) Gao, C., Mao, S., Kaufmann, G., Wirsching, P., Lerner, R. A., and Janda, K. D. (2002) A method for the generation of combinatorial antibody libraries using pIX phage display. *Proc. Natl. Acad. Sci. U.S.A. 99*, 12612−12616.

(21) Malik, P., Terry, T. D., Gowda, L. R., Langara, A., Petukhov, S. A., Symmons, M. F., Welsh, L. C., Marvin, D. A., and Perham, R. N. (1996) Role of capsid structure and membrane protein processing in determining the size and copy number of peptides displayed on the major coat protein of filamentous bacteriophage. *J. Mol. Biol. 260*, 9−21.

(22) Beckett, D., Kovaleva, E., and Schatz, P. J. (1999) A minimal peptide substrate in biotin holoenzyme synthetase-catalyzed biotinylation. *Protein Sci. 8*, 921−929.

(23) Steiner, D., Forrer, P., Stumpp, M. T., and Plückthun, A. (2006) Signal sequences directing cotranslational translocation expand the range of proteins amenable to phage display. *Nat. Biotechnol. 24*, 823−831.

(24) Day, L. A. (1969) Conformations of single-stranded DNA and coat protein in fd bacteriophage as revealed by ultraviolet absorption spectroscopy. *J. Mol. Biol. 39*, 265−277.

(25) Endemann, H., and Model, P. (1995) Location of filamentous phage minor coat proteins in phage and in infected cells. *J. Mol. Biol. 250*, 496−506.

(26) Guzman, L. M., Belin, D., Carson, M. J., and Beckwith, J. (1995) Tight regulation, modulation, and high-level expression by vectors containing the arabinose PBAD promoter. *J. Bacteriol. 177*, 4121−4130.

(27) Scheinberg, D. A., Villa, C. H., Escorcia, F. E., and McDevitt, M. R. (2010) Conscripts of the infinite armada: systemic cancer therapy using nanomaterials. *Nat. Rev. Clin. Oncol. 7*, 266−276.

(28) Kelly, K. A., Waterman, P., and Weissleder, R. (2006) In vivo imaging of molecularly targeted phage. *Neoplasia 8*, 1011−1018.

(29) Clark, C. J., and Sage, E. H. (2008) A prototypic matricellular protein in the tumor microenvironment−where there's SPARC, there's fire. *J. Cell. Biochem. 104*, 721−732.

(30) Hwang, J.-H., Lee, S. H., Lee, K. H., Lee, K. Y., Kim, H., Ryu, J. K., Yoon, Y. B., and Kim, Y.-T. (2009) Cathepsin B is a target of Hedgehog signaling in pancreatic cancer. *Cancer Lett 273*, 266−272.

(31) Chirico, N., Vianelli, A., and Belshaw, R. (2010) Why genes overlap in viruses. *Proc. Biol. Sci. 277*, 3809−3817.

(32) Specthrie, L., Bullitt, E., Horiuchi, K., Model, P., Russel, M., and Makowski, L. (1992) Construction of a microphage variant of filamentous bacteriophage. *J. Mol. Biol. 228*, 720−724.

(33) Herrmann, R., Neugebauer, K., Pirkl, E., Zentgraf, H., and Schaller, H. (1980) Conversion of bacteriophage fd into an efficient single-stranded DNA vector system. *Mol. Gen. Genet. 177*, 231−242.

(34) Huang, Y., Chiang, C.-Y., Lee, S. K., Gao, Y., Hu, E. L., De Yoreo, J., and Belcher, A. M. (2005) Programmable assembly of nanoarchitectures using genetically engineered viruses. *Nano Lett. 5*, 1429−1434.

(35) Bar, H., Yacoby, I., and Benhar, I. (2008) Killing cancer cells by targeted drug-carrying phage nanomedicines. *BMC Biotechnol. 8*, 37.